

# Nonlinear photonic structures for all-optical deflection

Tal Ellenbogen\*, Ayelet Ganany-Padowicz, Ady Arie

Department of Physical Electronics, Faculty of Engineering, University of Tel-Aviv, Tel-Aviv 69978, Israel

\*Corresponding author: [ellenbog@post.tau.ac.il](mailto:ellenbog@post.tau.ac.il)

**Abstract:** We present a new type of photonic structures in quadratic nonlinear materials that enable efficient and continuous all-optical deflection. The structures are based on two-dimensional modulation of the nonlinear coefficient and consist of a set of symmetric or anti-symmetric arcs that form a periodic pattern in the propagation direction and a chirped pattern in the transverse direction. Stoichiometric lithium tantalite structures were tested by second harmonic generation. Varying the pump wavelength from 1545 nm to 1536 nm resulted in continuous angular deflection of the second harmonic wave up to  $\sim 2.3^\circ$ . Continuous deflection was also obtained by varying the crystal temperature at a fixed pump wavelength.

©2008 Optical Society of America

**OCIS codes:** (230.1150) All-optical devices; (190.4223) Nonlinear wave mixing; (190.4360) Nonlinear optics, devices; (060.1155) All-optical networks.

---

## References and links

1. M. M. Fejer, G. A. Magel, D. H. Jundt, and R. L. Byer, "Quasi phase matched second harmonic generation: Tuning and tolerances," *IEEE J. Quantum Electron.* **28**, 2631-2654 (1992).
2. V. Berger, "Nonlinear photonic crystals," *Phys. Rev. Lett.* **81**, 4136-4139 (1998).
3. A. Arie, N. Habshoosh, and A. Bahabad, "Quasi phase matching in two-dimensional nonlinear photonic crystals," *Opt. Quantum Electron.* **39**, 361-375 (2007).
4. S. Zhu, Y. Y. Zhu, and N. B. Ming, "Quasi-phase-matched third-harmonic generation in a quasi-periodic optical superlattice," *Science* **278**, 843-846 (1997).
5. K. Fradkin-Kashi, A. Arie, P. Urenski, and G. Rosenman, "Multiple nonlinear optical interactions with arbitrary wave vector differences," *Phys. Rev. Lett.* **88**, 023903 (2002).
6. R. Lifshitz, A. Arie, and A. Bahabad, "Photonic quasicrystals for nonlinear optical frequency conversion", *Phys. Rev. Lett.* **95**, 133901 (2005).
7. A. Bahabad, N. Voloch, A. Arie, and R. Lifshitz, "Experimental confirmation of the general solution to the multiple phase matching problem," *J. Opt. Soc. Am. B* **24**, 1916-1921 (2007).
8. Y. Li, D. Y. Chen, L. Yang, and R. R. Alfano, "Ultrafast all-optical deflection based on an induced area modulation in nonlinear materials," *Opt. Lett.* **16**, 438-440 (1991).
9. G. Stegeman, D. Hagan, and L. Torner, " $\chi^{(2)}$  cascading phenomena and their applications to all-optical signal processing, mode locking, pulse compression, and solitons," *Opt. Quantum Electron.* **28**, 1691-1740 (1996).
10. S. M. Saltiel and Y. S. Kivshar, "All-optical deflection and splitting by second-order cascading," *Opt. Lett.* **27**, 921-923 (2002).
11. T. Pertsch, R. Iwanow, R. Schiek, G. I. Stegeman, U. Peschel, F. Lederer, Y. H. Min, and W. Sohler, "Spatial ultrafast switching and frequency conversion in lithium niobate waveguide arrays," *Opt. Lett.* **30**, 177-179 (2005).
12. V. R. Almeida, C. A. Barrios, R. R. Panepucci, and M. Lipson, "All-optical control of light on a silicon chip," *Nature* **431**, 1081-1084 (2004).
13. O. Limon, A. Rudnitsky, Z. Zalevsky, M. Nathan, L. Businaro, D. Cojoc, and A. Gerardino, "All-optical nano modulator on a silicon chip," *Opt. Express* **15**, 9029-9039 (2007).
14. T. Wang, B. Ma, Y. Sheng, P. Ni, B. Cheng, and D. Zhang, "Large-angle acceptance of quasi-phase-matched second-harmonic generation in homocentrally poled LiNbO<sub>3</sub>," *Opt. Commun.* **252**, 397-401 (2005).
15. D. Kasimov, A. Arie, E. Winebrand, G. Rosenman, A. Bruner, P. Shaier, and D. Eger, "Annular symmetry nonlinear frequency converters," *Opt. Express* **14**, 9371-9376 (2006).
16. Y. Furukawa, K. Kitamura, E. Suzuki, and K. Niwa, "Stoichiometric LiTaO<sub>3</sub> single crystal growth by double-crucible Czochralski method using automatic powder supply system," *J. Cryst. Growth* **197**, 889-895 (1999).
17. T. Ellenbogen, A. Arie, and S. M. Saltiel, "Non-collinear double quasi phase matching in one dimensional poled crystals," *Opt. Lett.* **32**, 262-264 (2007).
18. G. P. Agrawal, *Nonlinear Fiber Optics* (Academic, Boston, Mass., 1995).

19. A. Bruner, D. Eger and S. Ruschin, "Second harmonic generation of green light in periodically-poled stoichiometric LiTaO<sub>3</sub> doped with MgO," J. Appl. Phys. **96**, 7445-7449 (2004).
20. J. P. Torres, A. Alexandrescu, S. Carrasco, and L. Torner, "Quasi-phase-matching engineering for spatial control of entangled two-photon states," Opt. Lett. **29**, 376-378 (2004).

Nonlinear photonic crystals, in which the quadratic nonlinear coefficient is spatially modulated, are widely used to enable efficient three wave mixing interactions [1,2]. Many periodic [1-3], and quasi-periodic structures [4-7], have been used in recent years for phase matching collinear and non-collinear interactions. Most of these structures offer discrete phase matching solutions and can be used to generate optical radiation at a single and specific direction. In this work we present a new type of structures that offers continuous non-collinear phase matching possibilities, allowing continuous wavelength controlled all-optical deflection (AOD) which can be further tuned by adjusting the crystal temperature. These properties can be used to design and engineer new types of optical devices controlled solely by light.

All-optical data processing eliminates the need for optical-electrical-optical conversions in optical communication systems, thereby enabling simpler and faster systems. Therefore, a great effort has been made in recent years to the research and development of new types of all-optical processes and all-optical devices, e.g., AOD [8-10], and all-optical switching [11-13].

The method proposed in this paper to implement continuous AOD is based on nonlinear three wave mixing processes. Such processes in bulk materials suffer phase mismatch between the generating internal polarization wave and the generated optical radiation waves due to the dispersion of the material. These processes can be quasi phase matched by inverting the quadratic nonlinear coefficient in specific patterns [1,2]. An interaction can be phase matched by a modulated structure if there exists in the structure a reciprocal lattice vector (RLV) that is equal to the wave-vectors mismatch of the interacting waves, e.g., for second harmonic generation (SHG) the required RLV is:

$$\vec{k}_G = \vec{k}_2 - 2\vec{k}_1 \quad (1)$$

Where  $\vec{k}_1$  and  $\vec{k}_2$  are the wave vectors of the first and second harmonic waves respectively, and  $\vec{k}_G$  is the required RLV to phase match the interaction.

The RLV content of each pattern of modulation is represented by its Fourier transform. In order to find the correct effective RLVs that can phase match an optical interaction, the Fourier transform of the structure should not be applied to all the crystal, but only to the section where the pump beam propagates. Figure 1 shows three different structures and their respective wave-vector diagrams for a plane wave and for a finite beam. A one dimensional periodic modulation is shown on Fig. 1(a), where the phase matching possibilities are the same for the plane wave and the finite beam. These structures as well as periodic or quasi periodic two dimensional structures have discrete sets of RLVs, thus the generated second harmonic can propagate only in specific directions. The annularly poled structure, shown on Fig. 1(b), consists a continuous set of RLVs in a circular outline [14, 15] (Since RLVs are discrete by definition we will refer to the continuous set as quasi phase matching (QPM) vectors). However, in the case of a finite beam, the available phase matching possibilities are practically similar to the one-dimensional structure shown in Fig. 1(a). For this reason, annularly poled structures are not optimal for continuous non-collinear phase matching.

We introduce here patterns of modulation for the quadratic nonlinear coefficient that enable continuous non-collinear phase matching possibilities for finite beam width waves as shown in Fig. 1(c), which can be applied for a variety of AOD devices. The spatial modulation of the nonlinear coefficient to create a symmetric structure is described by:

$$\chi^{(2)}(x, y) = \text{sign}\{\cos[2\pi(f_x x + f_{yy} y^2)]\} \quad (2)$$

Where  $f_x=1/\Lambda$  is a fixed spatial modulation in the propagation direction with  $\Lambda$  as the spatial period, which can be adjusted to set the collinear phase matching criteria.  $f_{yy}$  is the transverse frequency gradient parameter which applies a linearly chirped frequency change in the transverse direction. This parameter can be adjusted to set the bandwidth of non-collinear phase matching solutions. Increasing  $f_{yy}$  will enlarge the deflection tolerance, but will reduce the efficiency. The linearly chirped nature of the transverse pattern of modulation was chosen since it consists of a continuous set of QPM vectors and results in a structure that is easy to realize. Other forms of transverse modulation, e.g. nonlinear chirped frequency change, can be applied for shaping the angular dependence of the deflection efficiency. The resulted structure contains arc shaped domains ordered in a periodic pattern in the propagation direction. Figures 2(a), 2(b) and 2(c) show three different periodic structures with their respective effective QPM vectors presented by their numerical Fourier transform: a one-dimensional structure ( $f_{yy}=0$ ), the proposed structure and its anti-symmetric version (where  $f_{yy}$  is multiplied by  $\text{sign}(y)$ ). It can be seen that the proposed structures offer a rich and continuous set of non-collinear phase matching possibilities. The interactions can be phase matched to both sides by using a symmetric structure or to one side by using an anti-symmetric structure. Since the duty cycle of the structures was chosen to be 50% only odd QPM vectors orders appear in the Fourier image (The 1<sup>st</sup> and 3<sup>rd</sup> orders are shown). The whole range of QPM vectors contained in the transverse axis of the structure is marked as transverse matching tolerance - TMT.

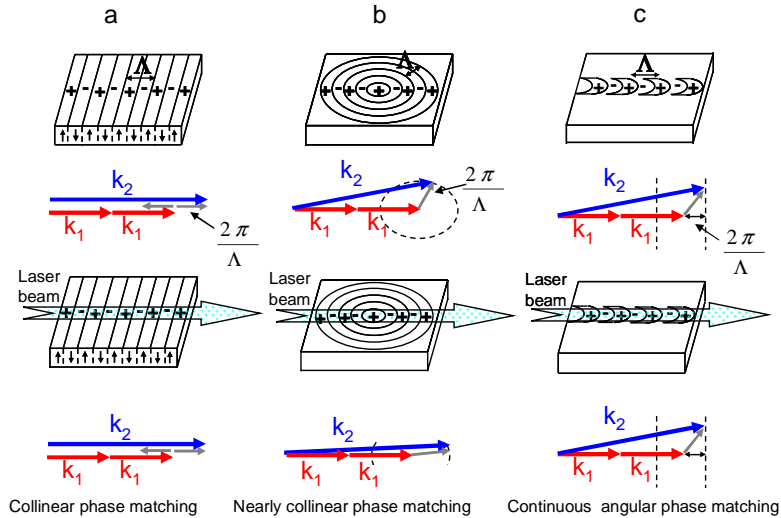


Fig. 1. Three schemes of nonlinear structures (top line), wave-vector diagrams for SHG processes of a plane wave (2<sup>nd</sup> line), schemes of a finite beam width wave propagating in the structures (3<sup>rd</sup> line) and the corresponding wave-vector diagrams (4<sup>th</sup> line) in: (a) one-dimensional periodically poled structure, (b) annularly poled structure, and (c) the proposed structure for continuous AOD.

Phase matching solutions for second harmonic generation, with the proposed structures are described by:

$$\cos \rho = \frac{2k_1 + G_m}{k_2} \quad (3)$$

Where  $G_m=2\pi m/\Lambda$ ,  $m$  is the QPM vectors order, and  $\rho$  is the internal angle of deflection of the second harmonic waves. Figure 2(d) shows the dependence of the internal deflection of the second harmonic waves on the pump wavelength, for structures with different periods.

The symmetric structure was realized in a 0.5mm thick z-cut stoichiometric lithium tantalite crystal, grown by the double-crucible Czochralski method [16], at Oxide Co. and doped with 0.5 mol % MgO. A structured pattern of photoresist was contact printed on the C+

face of the sample from a lithographic mask, and uniformly coated by a metallic layer. The electrical poling was achieved by applying 1 kV pulses to the crystal surfaces. The total switching charge was  $45 \mu\text{C}/\text{cm}^2$ . After poling, the photoresist and the metallic coatings were removed and the domain structure was revealed by HF etching.

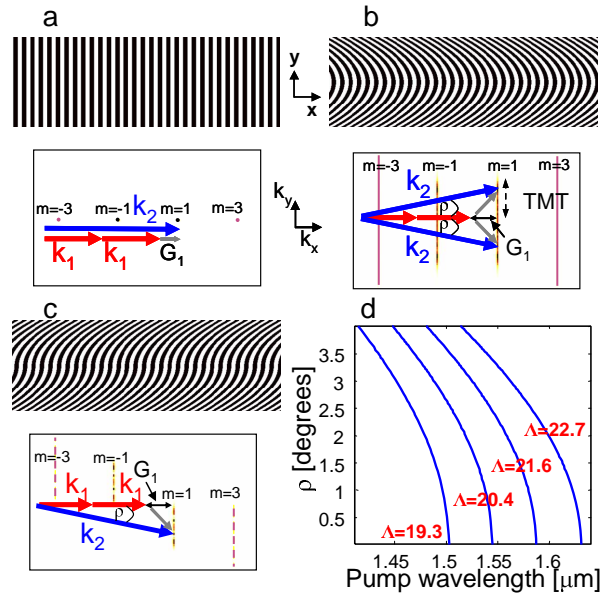


Fig. 2. (a)-(c). Three options for periodic structures, their numerical Fourier transform (3<sup>rd</sup> order vectors were color enhanced for viewing purposes) and first order vectorial phase matching schemes: (a) One-dimensional periodically poled structure, (b) The proposed symmetric structure and (c) The proposed anti-symmetric structure. (d) Wavelength dependence of the second harmonic deflection angle for continuous AOD structures with different periods  $\Lambda$  [ $\mu\text{m}$ ].

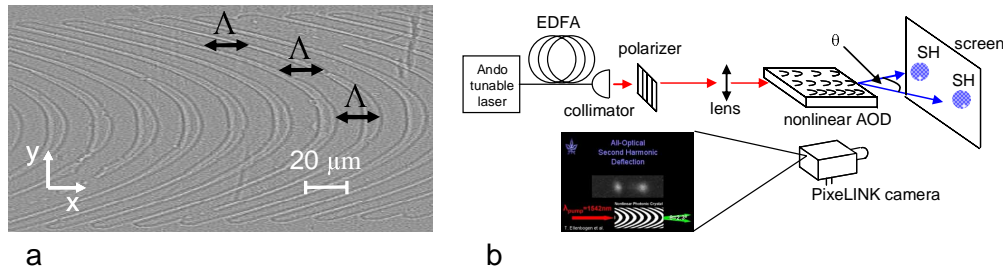


Fig. 3. (a). Microscope photograph of the  $\bar{C}$  side of the crystal, after selective etching (which reveals the inverted domain pattern). The Y axis was slightly resized for viewing purposes. The entire width of the channel is  $200 \mu\text{m}$ . (b) Experimental setup. Inset (1.5 MB) Movie of all-optical second harmonic deflection.

The manufactured structure consists of 15 different channels with periods in the propagation direction ranging from  $19 \mu\text{m}$  to  $23 \mu\text{m}$ . Each channel is  $200 \mu\text{m}$  wide and  $20 \text{mm}$  long. The transverse frequency gradient parameter  $f_{yy}$  is  $5 \times 10^{-4} \mu\text{m}^{-2}$  for all the channels. The TMT of these structures is  $0.075 \mu\text{m}^{-1}$  which is equivalent to  $3.24^\circ$  external deflection of the second harmonic wave by a  $1529 \text{nm}$  pump deflector. A microscope photograph of a channel in the etched structure is shown in Fig. 3(a). It can be seen that the structure is periodic in the propagation direction and chirped in the transverse direction.

A SHG experiment was performed to examine the deflection possibilities enabled by the structure. The experimental setup is plotted in Fig. 3(b). The deflector was placed in a temperature controlled oven and pumped with an Ando 4321D tunable laser source. The laser source was amplified by an Erbium doped fiber amplifier to produce 30-40 mW of coherent radiation and the pump polarization was set to the crystallographic C axis by a polarization controller and a polarizer. The pump beam was then focused to the crystal with a waist radius of 35  $\mu\text{m}$ . We varied the temperature of the crystal and the pump wavelength and recorded the respective second harmonic outputs with a pixeLINK camera and with an Ophir visible detector. The measured deflection angles were compared to theoretical deflection angles, calculated with Eq. (3) after considering Snell's law, and the measured intensities were compared to a split-step Fourier numerical simulation [17, 18], in which the input was a non-depleted single-mode Gaussian beam, having a waist radius of 35  $\mu\text{m}$  in the middle of a 20 mm long crystal. The nonlinear coefficient used for the simulation was  $d_{33}=13 \text{ pm/V}$  [19].

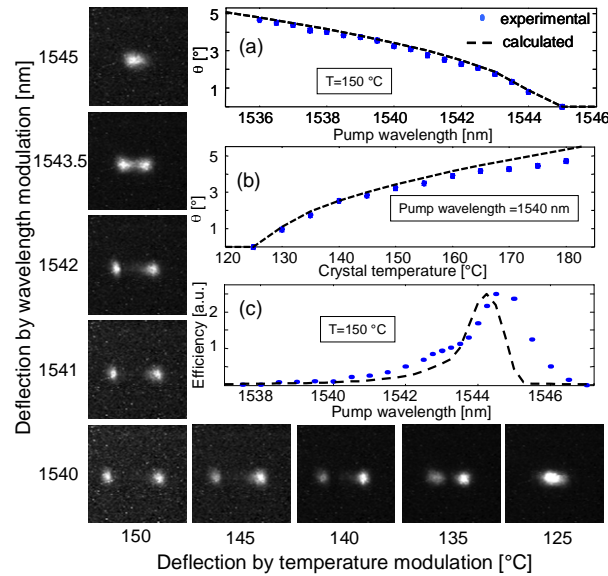


Fig. 4. Experimental (dots) and calculated (dashed line) deflection angle of the second harmonic as a function of (a) pump wavelength and (b) crystal temperature. (c) Normalized efficiency of the deflection process vs. pump wavelength. Photos on the left and bottom show the deflection of the second harmonic output for pump wavelength and crystal thermal modulation, respectively.

Figure 4 shows experimental and numerical results for all-optical deflection of the second harmonic output obtained by a symmetric structure with  $\Lambda=20.4 \mu\text{m}$ . The photographs on the left and bottom of Fig. 4, as well as the movie in Fig. 3(b), show the continuous wavelength and thermal dependent deflection as captured by our pixeLINK camera. Figures 4(a) and 4(b) show the dependence of the second harmonic deflection angle on wavelength and temperature. In these figures,  $\theta$  is the external angle between the two second harmonic spots as defined in Fig. 3(b). Varying the pump wavelength from 1545 nm to 1536 nm at 150 °C resulted in continuous angular deflection of the second harmonic wave up to  $\sim 2.3^\circ$ . Same results were obtained by varying the crystal temperature from 125 °C to 180 °C at 1540 nm pump wavelength.

Figure 4(c) shows the normalized measured and calculated efficiency curves for the process. The right and left regions of decline in efficiency in the curves are caused by different physical effects. It can be seen on Fig. 2(d) that the QPM vector content of the structure supports phase matching for pump waves at  $\sim 1544.5 \text{ nm}$  and in the near region below. Therefore, the right side decline of the curve shows the effect of going out of phase

matching for pump wavelengths above 1544.5 nm and the left side decline of the curve is due to the effect of the walk off of the interacting waves. Because of the fact that the SHG waves in the crystal are deflected, the interaction lengths decrease and the process becomes less efficient. Methods for walk-off compensation of the interacting waves can eliminate the left hand side of decline in efficiency.

The line shapes of the experimental and calculated results agree well both for the deflection angles and for the efficiency of the process. The peak calculated internal efficiency was  $0.233 \%W^{-1}$  and the peak measured internal efficiency, considering Fresnel reflection from both surfaces was  $0.051 \%W^{-1}$ . The difference in efficiency is reasonable, originated from structural defects in the manufactured crystal and due to the fact that the duty cycle of the periodic pattern is about 75% instead of the optimum 50%.

The ability to control the deflection angle of one light beam by another, in a nonlinear three wave mixing process, which is enabled by the structures presented in this paper, can be used in various AOD based devices, e.g. an optical scanner at the second harmonic of a tunable laser, or an all-optical router for optical telecommunication networks. Figure 5 shows a proposed configuration for an all-optical router using the nonlinear continuous AOD crystal presented here. This configuration includes a signal beam and a control beam. The generated sum frequency output will be deflected to the appropriate channel according to the control beam wavelength. In each channel the output will be mixed again with the control wavelength in a down conversion process, to go back to the frequency of the original information packet. This scheme for all optical routers can be applied in fiber-optics communications networks or in metropolitan and satellite free-space-optics networks.

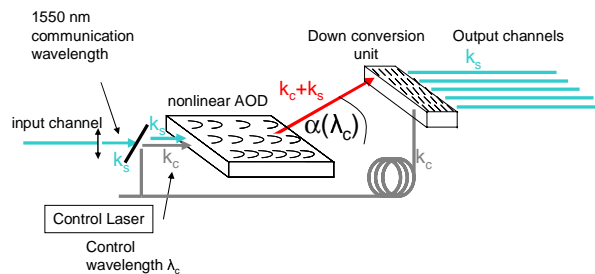


Fig. 5. A proposed configuration for an all-optical router using the presented nonlinear AOD crystal.

In summary, we have introduced in this paper nonlinear structures that enable continuous all-optical deflection by using three wave mixing processes. These structures can be adjusted, as far as crystal poling technology allows, to act as continuous all-optical deflectors at any chosen spectral band by adjusting the collinear phase matching criteria  $f_x$ . Desired bandwidths of non-collinear phase matching solutions can be fitted by adjusting the transverse frequency gradient parameter  $f_{yy}$ . The structures were tested in SHG experiment and continuous deflection of the second harmonic output from 0 degrees up to  $\sim 2.3$  degrees was recorded. The experimental results agree well with calculations. The structure presented in this paper shows continuous all-optical angular deflection which is more than two orders of magnitude larger than achieved in Kerr-induced deflectors [8]. The proposed structures can be used in fiber-optics or free-space-optics telecommunication networks, as they eliminate bottlenecks caused by intermediate conversion to electrical signals. Moreover, the proposed structures can be applied for applications such as scanning, unique generations of entangled photon states [20], or wavelength conversion and harmonic generation of ultra-short pulses.

### Acknowledgment

This work was supported by the Israeli Science Foundation, grant no. 960/05 and by the Israeli Ministry of Science. We thank Dr. David Eger and Pnina Shaier of Soreq NRC for their assistance in preparing the sample.